isvr Institute of Sound and Vibration Research

Wavenumber Estimation: Further Study of the Correlation Technique and Use of SVD to Improve Propagation Direction Resolution

A.N. Thite and N. S. Ferguson

ISVR Technical Memorandum No 937

June 2004

University of Southampton

SCIENTIFIC PUBLICATIONS BY THE ISVR

Technical Reports are published to promote timely dissemination of research results by ISVR personnel. This medium permits more detailed presentation than is usually acceptable for scientific journals. Responsibility for both the content and any opinions expressed rests entirely with the author(s).

Technical Memoranda are produced to enable the early or preliminary release of information by ISVR personnel where such release is deemed to the appropriate. Information contained in these memoranda may be incomplete, or form part of a continuing programme; this should be borne in mind when using or quoting from these documents.

Contract Reports are produced to record the results of scientific work carried out for sponsors, under contract. The ISVR treats these reports as confidential to sponsors and does not make them available for general circulation. Individual sponsors may, however, authorize subsequent release of the material.

UNIVERSITY OF SOUTHAMPTON

INSTITUTE OF SOUND AND VIBRATION RESEARCH

DYNAMICS GROUP

Wavenumber Estimation: Further Study of the Correlation Technique and Use of SVD to Improve Propagation Direction Resolution

by

A.N. Thite and N.S. Ferguson

ISVR Technical Memorandum No: 937

June 2004

Authorised for issue by
Professor M.J. Brennan
Group Chairman

CONTENTS

Wavenumber estimation: Further study of the correlation technique and use of SVD to improve propagation direction resolution.

1. INTRODUCTION

Techniques have been developed previously for the estimation of flexural wavenumbers and applied to wave propagation in one-dimensional structures such as beams [1-3] or in quasi-one dimensional structures such as cylinders [1] and tyres [4-5], where the motion for the latter is decomposed into essentially one dimensional components. Hence the direction of propagation is known or assumed. These methods include discrete Fourier Transforms [4], Prony series [1,5] and least squares methods [2,3]. Prony series approaches, in particular, seem to offer the most accurate estimation but are very sensitive to noise in the data and require equally spread data. The Fourier Transform technique requires equally spaced measurements and its wavenumber resolution is restricted by the size of the physical scan area in the same manner that the 'BT' product [6] restricting the frequency resolution B to the available length T of the data. Essentially most of the other aforementioned methods systematically fit complex exponential travelling waves to the measured data, from which the number of wave components present and their (complex) wavenumbers can be determined. In particular it is also possible to have an iterative procedure that fits to both the wavenumber and the wave amplitudes [1]. One could propose testing one-dimensional strips cut from a two-dimensional structure, but this is inapplicable for in-situ testing, in cases where there is curvature or for non-isotropic configurations. Furthermore this is not a true two-dimensional technique that is required for experimental validation of theoretical analyses [7].

There are substantial particular problems applying these methods to wave motion that is truly two-dimensional. These include resolution, noise, directionality, nearfields, cylindrical spreading and so on and, in general, the infinite headings on which the free waves may propagate through the structure. The most obvious difference in estimating the wavenumbers in two-dimensional structures is the large quantity of data required. It is difficult to obtain good quality, noise free data at all points and at all frequencies – occasional bad measurements are unavoidable. Thus it might be desirable, in whatever estimation process is adopted, to be able to weight the measured data according to a measure of its quality e.g. by the coherence. Furthermore, it may be difficult or impossible to measure responses at uniformly spaced

positions, so that techniques which require this are inapplicable. In principle a Prony series approach can be applied to two-dimensional structures (as suggested in reference [1]), but in practice the foregoing issues may make it impractical. Finally, in a finite structure with point excitation, there will be cylindrical spreading of the free waves and strong resonant behaviour will be exhibited if the modal overlap is low enough. At such frequencies certain wave components will dominate the response; their wavenumbers will be relatively easy to measure, but they will mask the presence of other (non-resonant) wave components. Thus the effectiveness of any proposed technique will be expected to depend on the modal overlap of the structure.

In [6] a general approach was described which aims to avoid or overcome some of the previous difficulties. Measurements of the mobility were taken on a flat isotropic and a flat anisotropic composite panel. An electrodynamic exciter was attached near to a corner and a broadband force excitation was applied. The transfer functions were subsequently obtained with measurements made over nominally equidistant grid points, using a scanning laser vibrometer. Here spatial correlation at each frequency between the measured locations was used to estimate the wavenumbers. Existence of wave propagation is indicated by large correlation at particular wavenumbers. However, it was observed that there can be ambiguity in the wavenumber estimation at resonances and missing information about the wave propagation in other directions. It was also suggested that using higher damping would reduce the nearfield waves at the boundaries. For further validation it was envisaged that if more wavenumber components could be resolved, e.g. because of high modal overlap (more wavenumber components), more structural configurations with different boundary conditions (estimation at same and/or different frequencies), larger panels or high edge damping, then more complete estimation of the wavenumber field would be achieved.

The present work further investigates the correlation technique in order to improve wavenumber directional resolution, estimation at resonances and comparison of the benefits of different test configurations. Initially the technique is briefly introduced [6], with some examples from earlier study. Later simulations on the free-free and simply supported plate have been used to understand the influence of different parameters on the resolution at low and high modal overlap. The singular value decomposition technique (SVD) is then used in resolving directions of wave propagations. Some additional experiments were performed on a curved

sandwich plate for validation purpose. Lastly a modified approach using the two dimensional correlation approach is suggested which can improve wave propagation direction resolution under certain conditions.

2. THE CORRELATION TECHNIQUE

The formulation used is given below [6] which has been implemented for a discrete number of points measurement points for a scan using the Cartesian co-ordinate system.

$$\hat{W}(k_{tx},k_{ty},\omega)=\int_{-l_x/2}^{l_x/2}\int_{-l_y/2}^{l_y/2} w(x,y,\omega)\,e^{-ik_{tx}x}\,e^{-ik_{ty}y}\,dxdy \tag{1}$$

where $\hat{W}(k_{tx},k_{ty},\omega)$ is correlation coefficient at wavenumber with components k_{tx} and k_{ty} with frequency ω, l_x and l_y are the dimensions of the nominally rectangular scan area and x and y are spatial locations on structure where response w is measured. The correlation coefficient will have peak values at particular wavenumber $k_t(k_{tx},k_{ty})$ vector. If wave propagation is equally likely in all directions, the peak value of correlation coefficient will occur at many combinations of k_{tx} and k_{ty}.

In practice the structural response, $w(x,y,\omega)$ available for analysis is not continuous in space. Usually it is sampled discretely at several spatial co-ordinates on the structure. This necessitates modification of equation (1) to sampled data. The modified formulation for the correlation coefficient is given by

$$\hat{W}(k_{tx},k_{ty},\omega)\cong\frac{l_x l_y}{N^2}\sum_{p=1}^{N}\sum_{q=1}^{N} w(x_p,y_q,\omega)e^{-ik_{tx}x_p}\,e^{-ik_{ty}y_q} \tag{2}$$

Sampling of the response at certain locations may have some implications on identification of wave propagation in structure under consideration. The parameters that influence the correlation for the presence of propagating waves (i.e. wavenumber and spatial dimensions) are k_{tx}, k_{ty}, N and the sampling locations x_p and y_p.

Simulations have been performed on a flat plate with simple supports and free edge boundary conditions, only flexural waves are considered. The general flexural wave equation in terms of transverse displacement, w, is given by

$$D\left[\frac{\partial^4 w}{\partial x^4}+2\frac{\partial^4 w}{\partial x^2 \partial y^2}+\frac{\partial^4 w}{\partial y^4}\right]=-\rho h\frac{\partial^2 w}{\partial t^2} \tag{3}$$

where $D=\frac{Eh^3}{12(1-\nu^2)}$, ν is the Poisson's ratio, E the Young's modulus of elasticity and ρ the density for the plate material. The following solution can be written for the above equation in terms of wave propagation at an angle θ to the **x** axis,

$$w(x,y,t)=Ae^{i(\omega t-k_x x-k_y y)} \tag{4}$$

where k_x and k_y are the wavenumbers in x and y directions respectively. These are related to wavenumber k by $k_x=k\cos\theta$ and $k_y=k\sin\theta$. Using (3) and (4),

$$\left[k_x^2+k_y^2\right]^2=k^2=\frac{\rho h\omega^2}{D} \tag{5}$$

The corresponding wavelengths in the two directions are given by

$$\lambda_x=\frac{2\pi}{k_x} \text{ and } \lambda_y=\frac{2\pi}{k_y} \tag{6}$$

A flat steel plate of size 915×590×1.6 mm^3 was used for the simulations. In general a damping loss factor of 1% percent has been used, except in the case study on increased damping and its effect on wavenumber resolution. Gaussian noise was added to the accelerances considered to achieve, to some degree, experiment like situation. The additive noise model used is

$$N(\omega)=C_1\omega N_{nd,1}e^{j2\pi N_{nd,1}}+C_2 N_{nd,2}e^{j2\pi N_{nd,2}} \tag{7}$$

where N_{nd} and N_{nu} are random numbers with normal and uniform distribution respectively and C are constants. The spatial mean accelerance for one of the simulated 'experiments' is shown in Figure 1. The fundamental mode occurs at around 16 Hz. The structure exhibits strong modal behaviour up to around 200 Hz. It is to be noted that the excitation was applied near the bottom left corner of the plate. The number of 'measurement' or sampling points used were 25 in the X

and in the 20 Y directions i.e. total of 500 points. The scan area was restricted to the smaller central part of the plate as shown in Figure 2 and its size is 0.36×0.285 m^2.

Wavenumber variation with frequency calculated using equation (5) is shown in Figure 3. This can be used in assessing accuracy of the estimates from the correlation technique. Figure 4 shows the corresponding wavelengths. This information will be used subsequently in explaining the performance of the correlation technique.

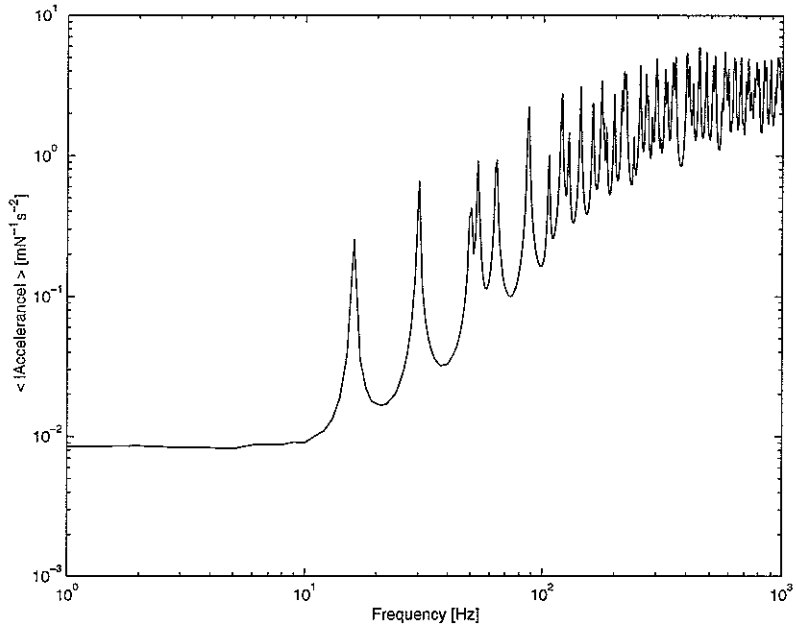

Figure 1. Simulated spatial mean accelerance on a simply supported flat rectangular plate with corner excitation.

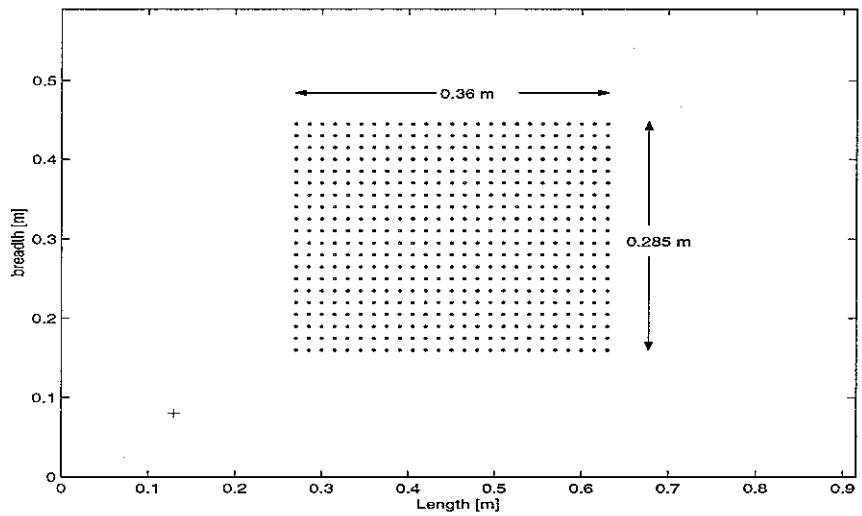

Figure 2. Small scan area used on the plate. Excitation point + is also shown.

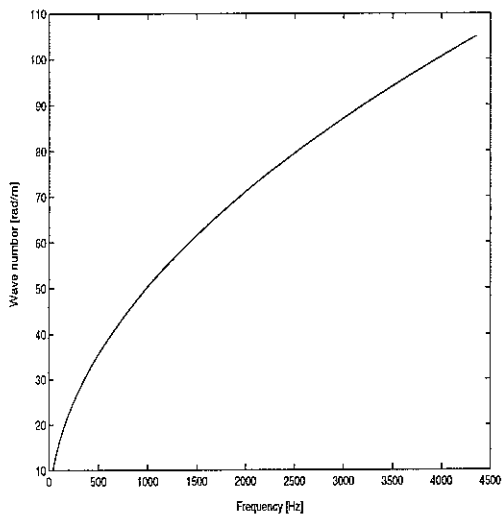

Figure 3. Wavenumber variation for a flat steel plate of 1.6 *mm thickness.*

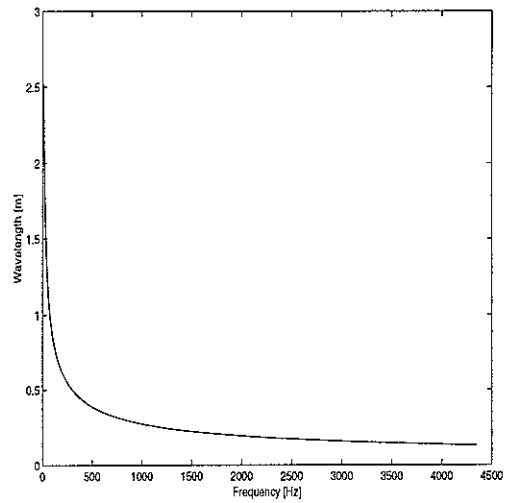

Figure 4. Wavelength variation for a flat steel plate of 1.6 *mm thickness.*

2.1. Wavenumber resolution

As in temporal signal processing, the spatial domain analysis also shows some constraints that need consideration in planning the measurements. One of the issues is the finest resolution that can be achieved with reasonable accuracy in any of wavenumber estimation. In this section the effect of sampling on resolution of the measured wavenumbers is discussed. In case of temporal data 1/T is the frequency resolution, where T is the time length of the measured sample. Similarly, in the case of the spatial domain the best wavenumber resolution is restricted by the size a dimension of the scan area to be $\frac{\pi}{a}$. Here half a wavelength is considered as this would still result in identification of the wavenumber by the presence of correlation peaks at multiples of that wavenumber. For the scan of Figure 2 this value is 9 rad/m.

The wavenumber estimation at 500 Hz is shown in Figure 5. Prominent contour centres are located at nearly two times the spatial resolution in the y direction and 3 times in the x direction. The wavenumber estimated is 35 rad/m which is very close to 35.6 rad/m given in Figure 3. The correlation shows lot of spreading (each contour area). It is interesting to note that only two directions of wave propagations are identified. The reasons for this could be coarse

resolution of the wavenumbers, predominant wave propagation in preferred directions or unknown sampling related issue.

In another simulated 'experiment' the scan area is increased whilst maintaining the same number of points and the excitation location so that there is improvement in resolution. The scan area covers almost the entire area of plate. The finest wavenumber resolution here is 3.7 rad/m. The wavenumbers estimated at 500 Hz for this case is shown in Figure 6. The correlation contours are closer than previously and more propagation directions are identified. However, it is still not possible to identify wavenumbers in many directions. It appears that resolution alone will not essentially improve wavenumber measurement. The wavenumber resolution is crucial at lower frequencies where wavenumbers are smaller. Here coarser resolution would result in a larger spread, where it may not be possible to distinguish different contours. If resolution were finer, it may be possible to distinguish different contours.

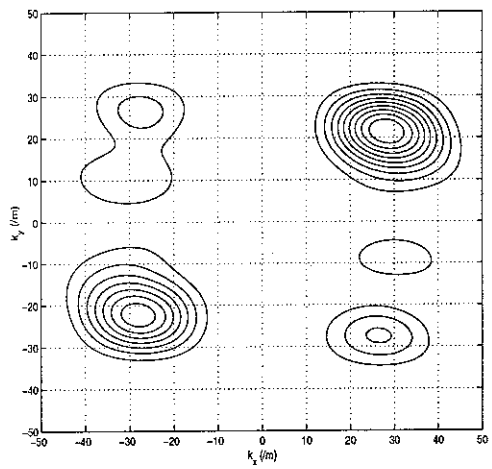

Figure 5. Wavenumber estimation at 500 Hz with corner excitation and limited scan area.

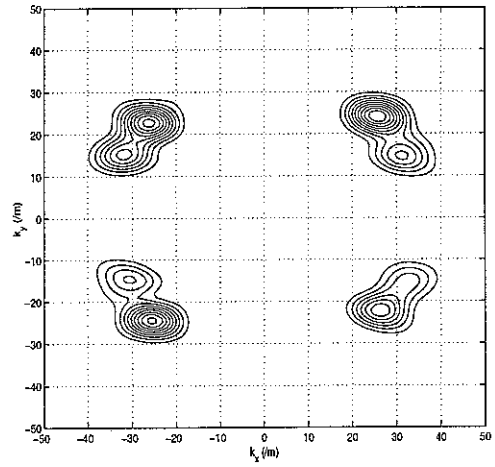

Figure 6. Wavenumber estimation at 500 Hz with corner excitation and large scan area.

It is obvious that at higher frequencies reasons other than resolution and preferential wave propagation directions are responsible for limited wavenumber identification. A possible reason is explained below. Re-examining equation (2), if one were to presume a direction of propagation, k_x and k_y would have a particular ratio for any wavenumber. It is also assumed that the energy due to direct field is dominant compared to reflected waves. The cylindrical spreading of waves will result in propagation of waves that will occur in several θ directions originating from the excitation point. Some of these directions are shown in Figure 7 for the

case under consideration. The correlation coefficient here will depend on how many points on the scan are crossed over by the propagating wave, which is dependent on the direction of wave propagation. It is most likely that directions closer to diagonal will have a larger number of crossed points. The number of points crossed over in some other directions can be very small. This means that depending on the wave propagation direction, the correlation coefficient calculated can vary significantly. This in turn would result in identification of only a few wave propagation directions. This is true even if the wave field is reverberant. This behaviour is seen in Figures 5 and 6 where contour centre locations correspond to directions that run closer to the diagonal in the example. This explanation also means that peaks of varying correlation coefficient that correspond to a wavenumber of interest may exist in most of the directions, but are masked by large coefficients in some specific directions. Improvements might be achieved with an alternative proper layout of scan points and location of excitation, in a polar co-ordinate scanned area.

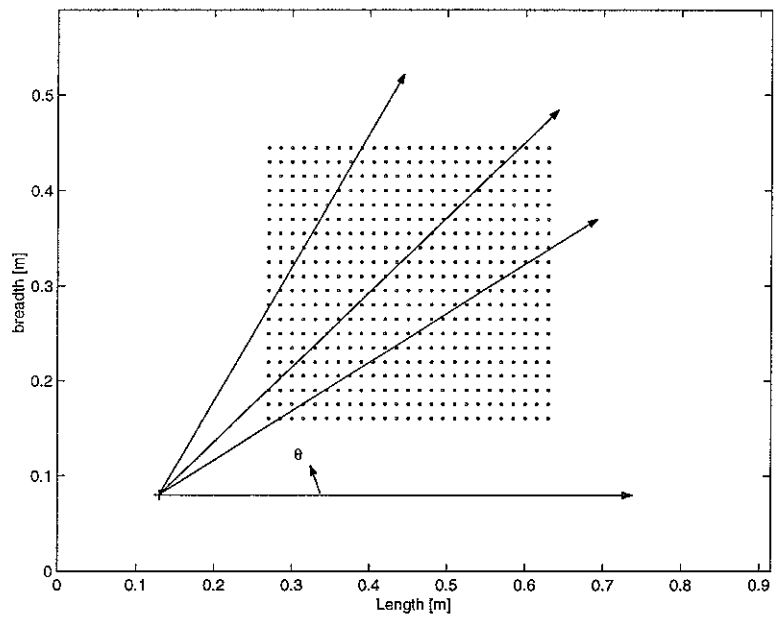

Figure 7. Small scan area along with some directions of wave propagation.

2.2. Effect of the location of the excitation point

In the measurement scan of Figure 2, travelling waves to the left and below the source are not captured directly. However, waves that are reflected from boundaries after crossing the scanning points are captured when moving to the left and towards the bottom of the plate. The

energy levels in the reflected waves can be smaller (depending on the damping) resulting in some contours not being prominently represented and masked by the larger correlation coefficients. Also as discussed earlier, a similar situation is encountered where corner excitation allows some directions of propagation crossing a larger number of points compared to others.

For the second case, excitation is applied at the centre of the plate instead of the corner. The scan areas remain as before. Figure 8 shows the wavenumber correlation at 500 Hz with the limited scan area. Although in most of the directions the number of scan points crossed over is similar, only four significant contours are seen in the plot. Nearly six independent contours were identified under corner excitation case (Figure 5), but the correlation intensity was varying for all of them. For centre excitation, however, the correlation is seen to be strong at all four locations. Here a limited number of wavenumbers are identified as the resolution is coarse (18 rad/m) compared to earlier case as the total span in each direction is reduced by a half. Coarser resolution means a spread in the correlation coefficient, hence a smaller number of prominent peaks. Figure 9 shows results for the larger scan area. Here it appears to identify a greater number of contours hence more travelling waves. By contrast, the correlation coefficient levels differ significantly across all contours. The contours appear to occur in pairs as expected for this case. When compared to corner excitation (Figure 5) where eight correlation contours were at larger levels, there appears to be little extra information. The wavenumber resolution here is 7.4 rad/m compared to 3.7 rad/m in corner excitation.

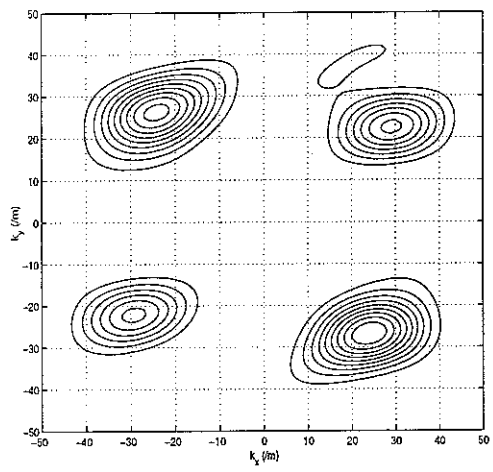

Figure 8. Wavenumber estimation at 500 Hz with centre excitation and limited scan area.

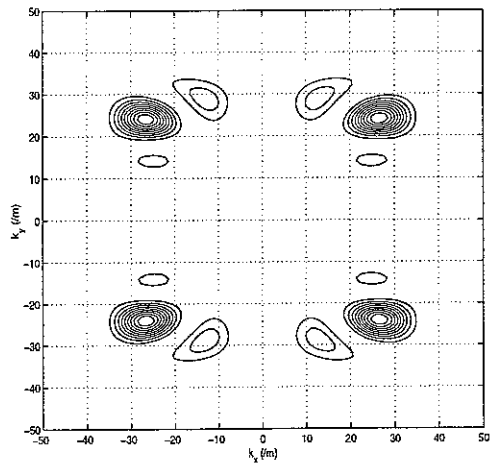

Figure 9. Wavenumber estimation at 500 Hz with centre excitation and large scan area.

It can be argued that if the excitation is near the corner, the waves travelling from one quadrant cross over a larger number of points compared to centre excitation. A smaller scan area, however, would reduce the segment of the angle of incidence of the travelling waves for corner excitation. To overcome this difficulty the excitation point needs to be closer to the scan area corner. If the waves are reflected efficiently at the boundaries, travelling waves in the opposite directions could also be identified with corner excitation. In the case of centre excitation, equal weighting (similar number of points crossed over in each direction) is given to wave propagation in all directions provided the wavefield is direct rather than modal or reverberant. The pairs of contours will hence be identified in each direction. Ideally, with a large scan area centre excitation would result in better wavenumber identification.

2.3. Effect of damping

Damping in the structure controls the energy associated with travelling waves in the spatial domain. Presence of larger damping is expected to reduce the energy associated with travelling waves as the distance travelled increases. This effect can have large implications on the wavenumber estimation procedures. In the above studies a structural damping loss factor of 1% has been used throughout. To study the influence of damping, a simulation with 10% damping loss factor was implemented for the large scan area case. The spatial mean accelerance is shown in Figure 10 for corner excitation. Strong modal behaviour is seen below only about 100 Hz.

Figure 11 shows wavenumber correlation contours at 500 Hz for larger damping and corner excitation. The process appears to prominently identify only one negative wavenumber in the x direction and a positive wavenumber in the y direction. This shows reduced reflection from the boundaries as most of travelling waves die out or contain reduced energy in the process of reaching the boundaries. This situation is expected to result in very little information on travelling waves which lie in the other 3 quadrants hence small correlation coefficients. Figure 12 shows a corresponding result for centre excitation. In this case the correlation process appears to identify more information with larger damping (compare with Figure 9). In Figure 9 it is possible that strong reflection of some waves may have created larger correlation coefficients at certain wavenumbers, possibly the standing wave patterns (modes), reducing the relative significance of some other waves. On the other hand, increased damping might allow

for equal representation for the free bending waves. The combination of centre excitation with larger damping can work better for the same number of 'measurement' points and scan area as in corner excitation. The resolution effect can also be seen in Figure 12 where in the x direction the analytical wavenumber equal to 35 rad/m cannot be identified as resolution is 7.4 rad/m (closest estimation at 37 rad/m). This results in energy being shared between contours centred at 37 and 29.6 rad/m, the largest correlation peak being the fomer.

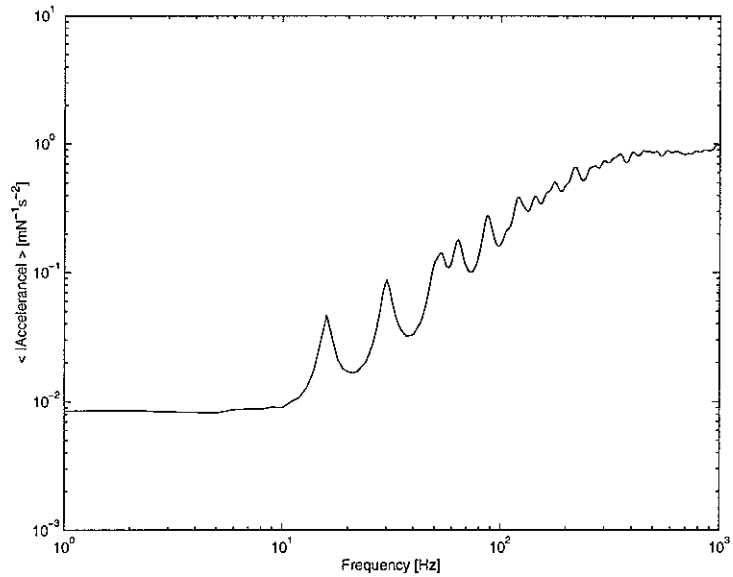

Figure 10. Spatial mean accelerance on a simply supported flat rectangular plate with corner excitation. The damping loss factor used is 10%.

2.4. Limitations on the maximum and minimum accurate wavenumber

In earlier sections the influence of measurement resolution on wavenumber estimate was studied. At the other end of the analysis, spacing between the scan points is expected to influence the maximum accurate wavenumber estimation. This influence is studied by omitting two lines of scans alternately, resulting in separation of the scanned lines equal to 0.115 m. This will result in maximum accurate estimate of wavenumber as 55 rad/m i.e. $\left(\frac{2\pi}{0.115}\right)$. Wavenumbers smaller than this allows for at least 2 scan points in a wavelength. Above the frequency that corresponds to the wavenumber of 55 rad/m, a mirror image of one half of the correlation contours occur i.e. spatial aliasing takes place. The wavenumber estimation at 800 Hz is shown in Figure 13 which confirms the above limitation. If the original scan is used, the

maximum accurate estimate of wavenumber increases to 165 rad/m. The corresponding correlation coefficient plot is shown in Figure 14. Although the resolution effect is still present, the mirror images disappear eliminating ambiguity in the wavenumber estimation.

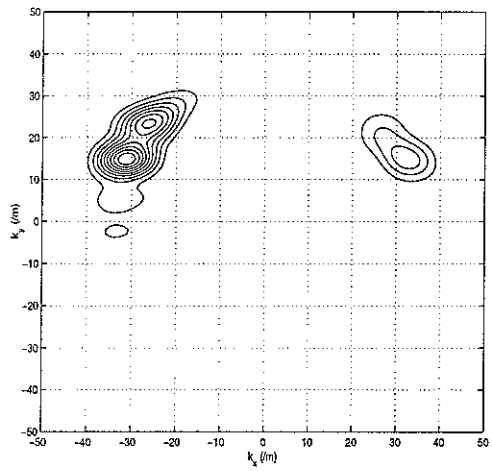

Figure 11. Wavenumber estimation at 500 Hz with corner excitation and limited area scan. Damping loss factor of 10% is used.

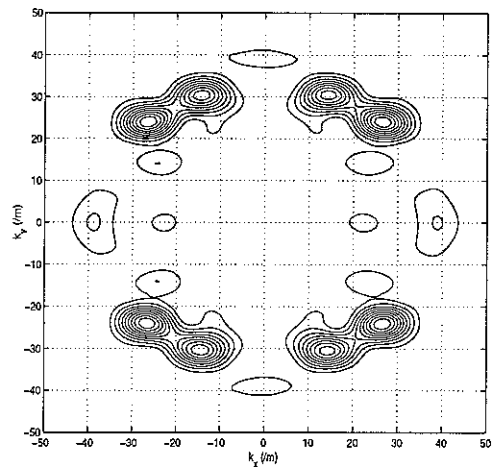

Figure 12. Wavenumber estimation at 500 Hz with centre excitation and limited area scan. Damping loss factor of 10% is used.

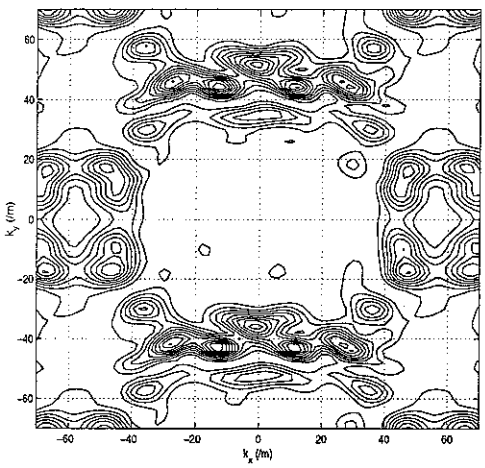

Figure 13. Wavenumber estimation at 800 Hz with corner centre excitation and large area scan with two alternate scan lines omitted. Damping loss factor of 10% is used.

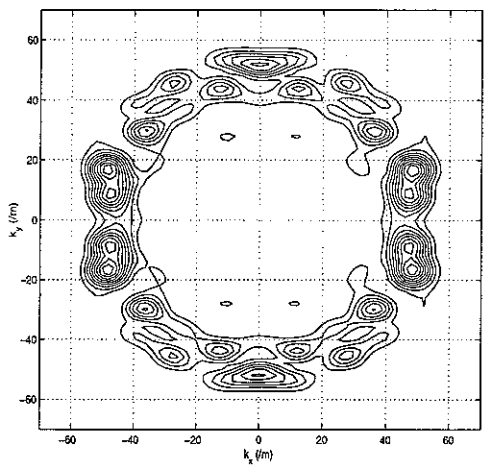

Figure 14. Wavenumber estimation at 800 Hz with centre excitation and large area scan. Damping loss factor of 10% is used.

A low wavenumber estimation limit using the correlation technique is given by $\left(\frac{2\pi}{\min(a,b)}\right)$. For wavenumbers smaller than this and scan length covering at least half a wavelength, the correlation coefficient will contain a peak at the proper wavenumber and several peaks of smaller values at multiples of it. This still allows accurate estimate of the wavenumber. When the scan length is smaller than half a wavelength, it can be considered to contain rigid body motion superimposed on the wave that is smaller in length than the actually propagating wave. This effect can be visualized using Figure 15.

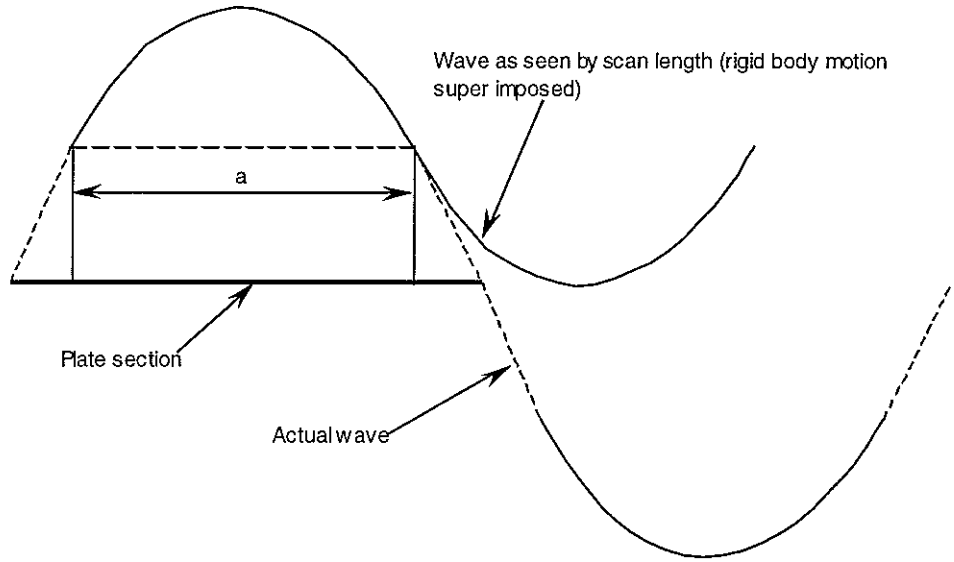

Figure 15. Section of plate when moving in first mode.

The rigid body motion contribution will have major influence on the estimated correlation coefficients. The motion can be treated as a rectangular signal in the spatial domain, extending across the dimensions of the scan area. In analogy to temporal signal processing, this signal is expected to have a broad band representation in wavenumber domain. The correlation coefficient of the broad band representation is given by $\frac{Al_x \sin(k_x x)}{k_x x}$, where A is the amplitude of the rectangular spatial movement. Graphically, a typical plot of this is given in Figure 16. Generally the first lobe dominates this signal, which indicates the presence of a high intensity contour at the centre of correlation coefficient plot.

For example at 16 Hz, the fundamental mode of the simply supported plate, the wavenumber estimated using correlation technique is shown in Figure 17. Here, only the contour centred on the zero wavenumber is identified. Which indicates prominence of 1st lobe in Figure 16. The propagating wave, which affects the correlation coefficient at the multiples of the wavenumber, are seen here to be masked by the correlation of the zero wavenumber component.

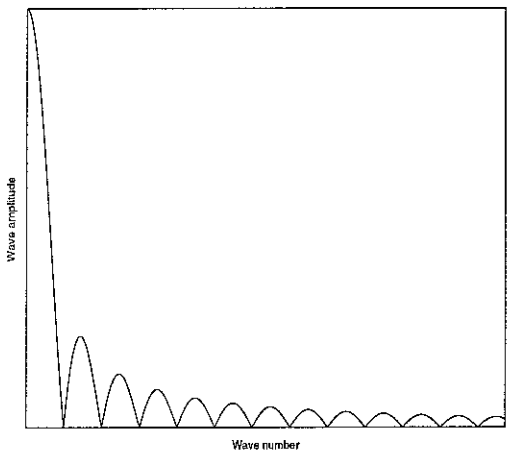

Figure 16. Wavenumber distribution for rigid body like motion.

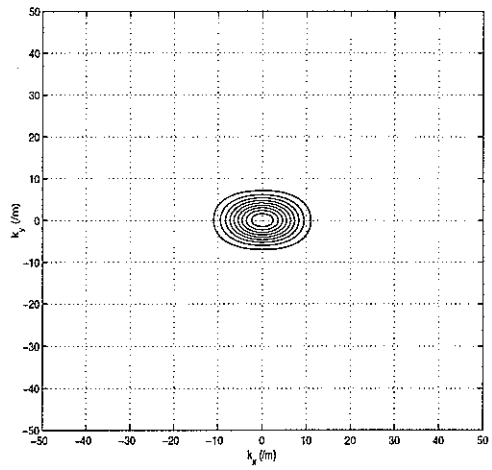

Figure 17. Wavenumber estimation at 16 Hz with corner excitation on simply supported plate and large area scan. Damping loss factor of 1% is used.

In all the cases considered above, simple supports has been assumed where nearfield waves at the plate edges do not occur. In experimental tests, however, it may not possible to achieve simple supports. In practice it is usually free-free supports. In such a situation near-field waves will be present at the boundaries of the structure. The presence of near-field waves may in addition have influence on the wavenumber estimation. The near-field wave decay rate is controlled by the wavenumber itself. As the wavenumber increases, the spatial distance within which nearfield waves decay decreases. Analogous to time v/s frequency domain, finer sampling in spatial domain means a wider wavenumber domain. For example, an exponentially decaying near-field wave can have wavenumber distribution (only one sided is shown) as

shown in Figure 18. The correlation coefficients are also seen to decay exponentially in this case.

At 500 Hz, with a limited scan area on the free-free plate results of wavenumber estimation are shown in Figure 19. Compared to Figure 5, the pattern of contours is significantly different. Also present are some other contours, although at lower correlation levels. Presence of these may be explained by the earlier arguments. As the frequency increases, nearfield waves are expected to have very small correlation coefficients in comparison to the travelling waves. Hence they are expected to have little influence on the wavenumbers estimated.

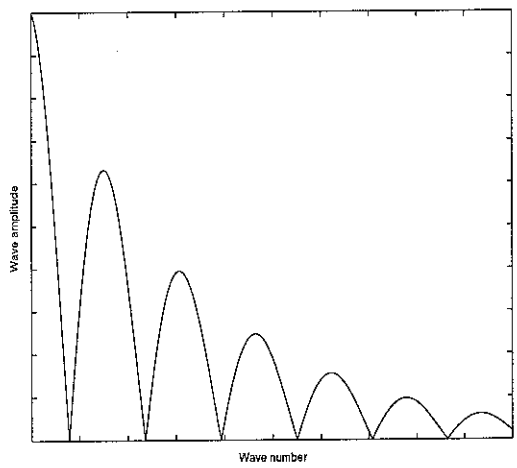

Figure 18. Wavenumber distribution for near-field waves.

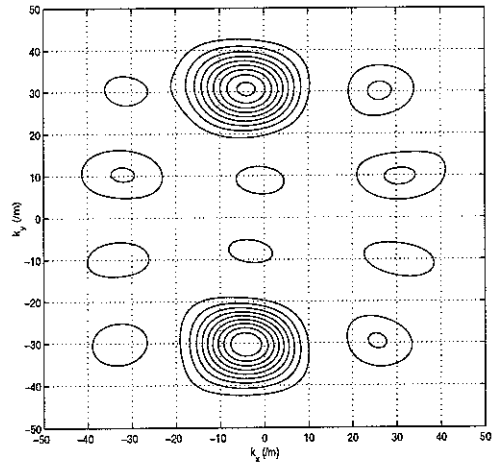

Figure 19. Wavenumber estimation at 500 Hz with corner excitation on free-free plate and limited area scan. Damping loss factor of 1% is used.

2.5. Discussion

The correlation technique when applied to sampled data appears to have certain limitations in its current form. These limitations are not only due to sampling. The excitation location, scan area and damping also appear to have influence on the accuracy of the wavenumbers estimates. A most critical limitation is that of identification of only a few directions of wave propagation at any frequency. Among others, this was seen to be primarily dependent on number of scan points crossed by each travelling wave. Although by proper planning each direction of propagation can be made to contain a similar number of scan points,

it is difficult to achieve this in practice. In the next section an alternative approach based on singular value decomposition is used to remove the masking effect of large correlation coefficients present in the scan.

3. USE OF SVD TO IMPROVE DIRECTIONAL RESOLUTION

A mobility or accelerance matrix $w(x, y, \omega)$ at any frequency can be written in terms of its singular values and unitary vectors. Using singular value decomposition, w can be written as

$$w(x, y, \omega) = USV^{H} \tag{7}$$

where S is a diagonal matrix of singular values, U and V are unitary matrices. Each singular value of the accelerance matrix contributes partially in forming the matrix. Writing $\lfloor w_{ij} \rfloor_k = U_{ik} s_k V_{kj}^H$ for j, k=1.....n and i=1.....m, then $[w] = \sum_k [w]_k$. The relative amplitudes of the singular values indicate the intrinsic relationships between elements of matrix. In the case of dominance of a particular mode, one of the singular values will appear larger compared to the others. The contribution to the FRF matrix by this singular value is expected to contain mostly the information about the dominant mode. Even if the wavefield is reverberant i.e. larger modal overlap, presence of a larger number of points in certain directions compared to others can also result in related elements in the response matrix. If wavenumbers are estimated using partial matrices, it might be possible to isolate the effect of dominant wave propagation direction or waves relating to larger correlation coefficients allowing identification of wavenumbers in other directions.

One of the accelerances estimated after the addition of noise using (6) is shown in Figure 20. The corresponding accelerance without noise is also shown in the figure. Below around 1000 Hz the structure has strong modal behaviour. Singular values of the accelerance matrix at each frequency are shown in Figure 21. The effect of noise is seen predominantly at some off-modal frequencies, there is hardly any influence at resonances. Only the first two singular values are not affected by noise at the lower frequencies. Due to increased modal overlap the dominance of the first few singular values reduces with frequency.

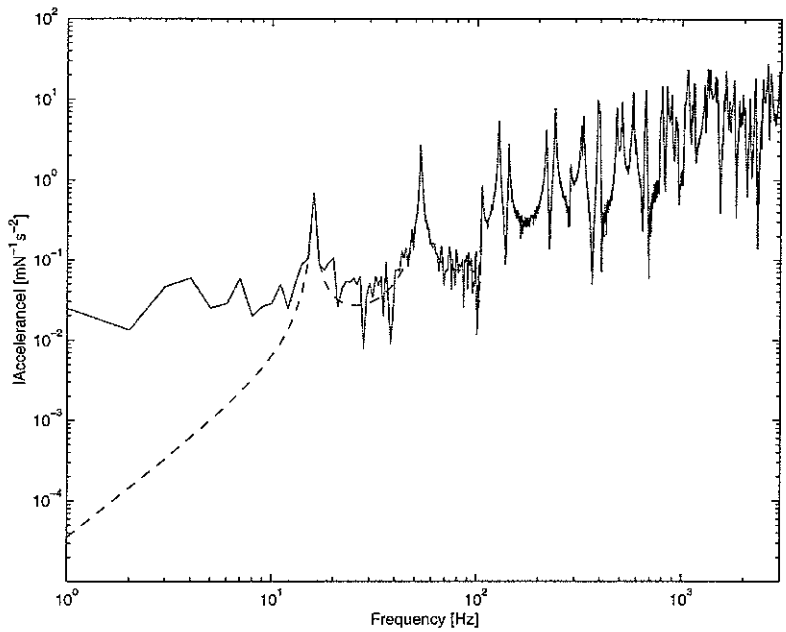

Figure 20. Typical transfer accelerance on simply supported plate with 1% damping loss factor and excited at the centre.

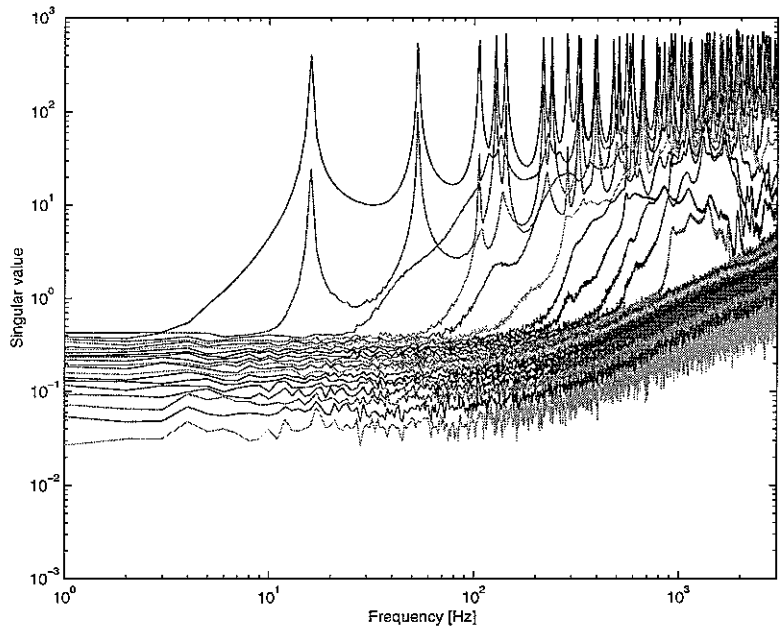

Figure 21. Singular values of FRF matrix for simply supported plate with 1% damping loss factor and excited at the centre.

The first singular values contribution to correlation coefficient at 16 Hz is same as that in Figure 17. The second singular value at this frequency results in a correlation contour that appears at multiples of the wavenumber resolution, which are due to side lobes in figure 16. Figure 22 shows the wavenumber correlation estimated using the partial contribution from the third singular value. Only this singular value appears to contain some further useful information. Even this estimate is larger than the actual wavenumber at that frequency. From this discussion it can be concluded that it is still difficult to estimate wavenumbers at frequencies where rigid body like motions dominate.

The calculations at the second mode i.e. 53 Hz are shown in Figures 23-26. At this frequency the first two singular values are dominant as seen from Figure 21. If singular value decomposition were not used, the correlation would appear as in Figure 23, which is actually the contribution from the first singular value alone. The first singular value here is dominated by flexural motion in contrast to rigid body like motion at 16 Hz. The contribution from rigid body motion is seen as a small contour at the centre. The rigid body like motion, however, appears to influence the second singular value as seen from Figure 24. The pattern of the correlation contours corresponds to side lobes in Figure 16. The use of singular value decomposition at 53 Hz leads to extraction of more information as seen from Figure 26. Wavenumbers are identified in more directions compared to the full FRF matrix calculations. Limitation of wavenumber resolution results in values that are different for the X and Y directions.

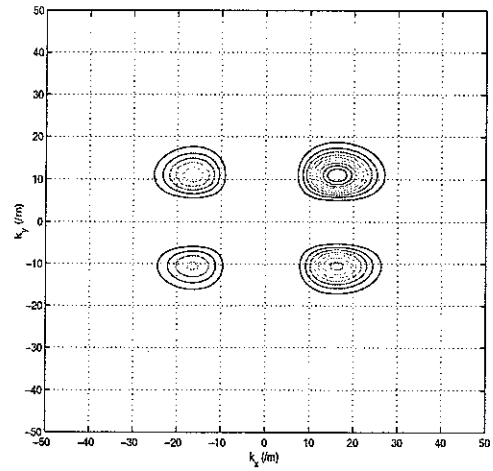

Figure 22. Third singular value contribution to wavenumber estimation at 16 Hz with centre excitation on simply supported plate with damping loss factor of 1% and large area scan.

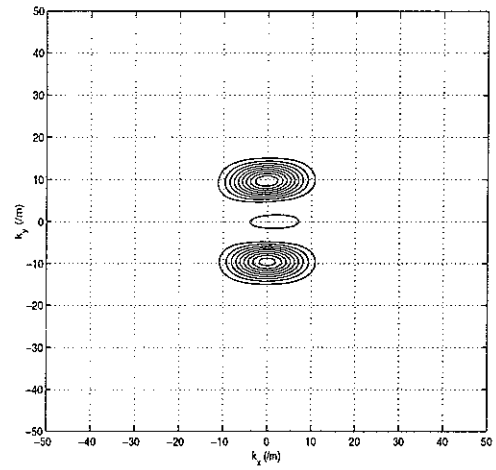

Figure 23. First singular value contribution to wavenumber estimation at 53 Hz with centre excitation on simply supported plate with damping loss factor and large area scan.

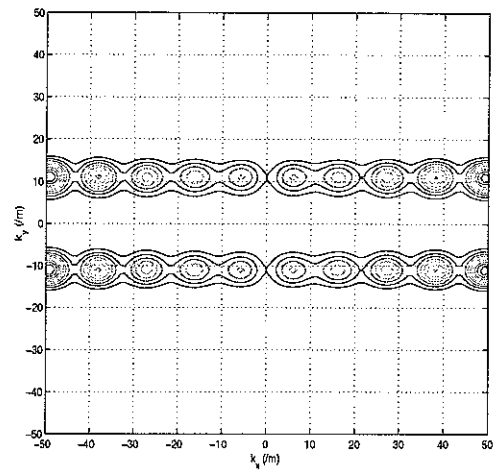

Figure 24. Second singular value contribution to wavenumber estimation at 53 Hz with centre excitation on simply supported plate with damping loss factor and large area scan.

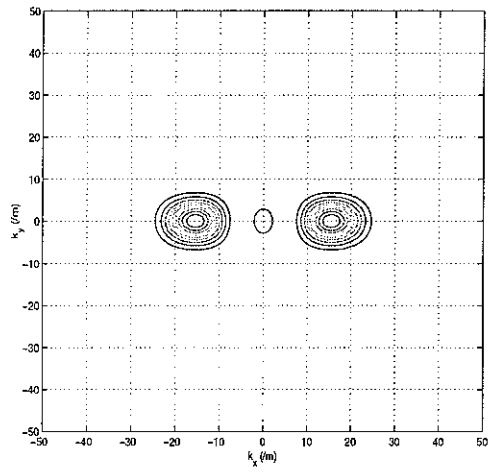

Figure 25. Third singular value contribution to wavenumber estimation at 53 Hz with centre excitation on simply supported plate with damping loss factor and large area scan.

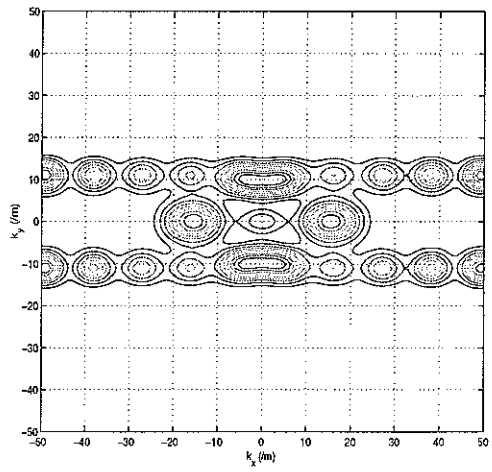

Figure 26. Summation of normalised contribution from first three singular values in estimating wavenumber estimation at 53 Hz with centre excitation on simply supported plate with damping loss factor and large area scan.

The process of considering singular value decomposition for estimating wavenumbers definitely helps in identifying more wavenumbers in different propagation directions at low frequencies as seen above. The question posed being, is it helpful at frequencies where more modes contribute significantly to the FRF anyway? For example, at 500 Hz nearly 7 singular values are quite similar in amplitude indicating good participation from many modes. But these singular values are distinguishable from each other indicating some intrinsic dependence of elements of the mobility matrix at this frequency. This might prove to be a hindrance as in the low frequencies. For further investigation analysis is carried out at 500 Hz.

The wavenumber correlation at 500 Hz due to contribution from the first singular value is shown in Figure 27. It shows the presence of contours at four locations which were also present in Figure 6. If the information of the first singular value is removed from the mobility matrix and correlation is then performed, the correlation contours look as in Figure 28. This figure shows 6 prominent locations of contours which can be extracted. These contours are more than were seen in Figure 6. Figure 29 shows correlation contours for contribution from the second singular value. This extracts information for wavenumbers in four more directions. The effect of removing the contribution from the first two singular values is shown in Figure 30. Here extra information appears about wavenumbers with x direction values being zero. The third singular value here extracts wavenumbers in two more directions out of four possible as shown in Figure 31. The combined effect of the first three singular values is shown in Figure 32. When compared to Figure 6, more number of contours are present and the locations appear to be more clearly defined i.e. actual location of the centres of the contours. This analysis supports the usefulness of singular value decomposition even at higher frequencies. However, it is not known a priori how many singular values would be significant.

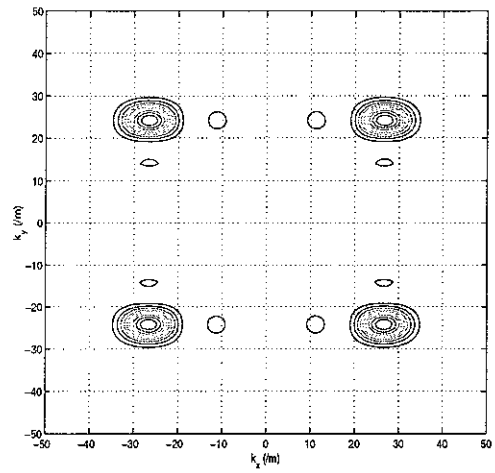

Figure 27. First singular value contribution to wavenumber estimation at 500 Hz with centre excitation on simply supported plate with damping loss factor and large area scan.

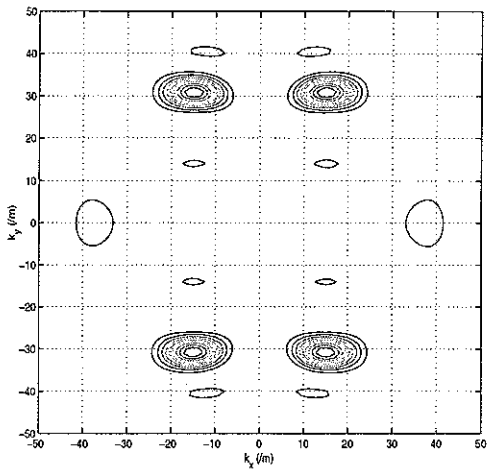

Figure 28. Contribution from all singular values except first one to wavenumber estimation at 500 Hz with centre excitation on simply supported plate with damping loss factor and large area scan.

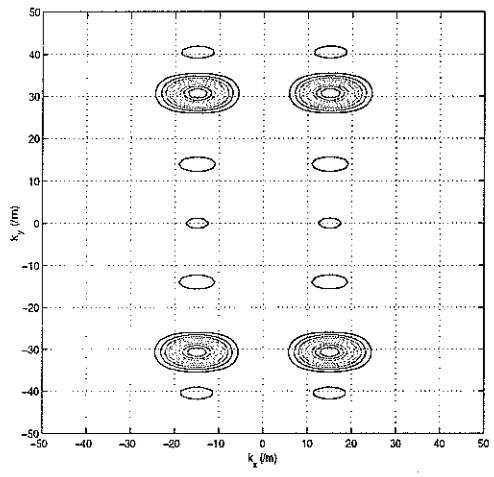

Figure 29. Second singular value contribution to wavenumber estimation at 500 Hz with centre excitation on simply supported plate with damping loss factor and large area scan.

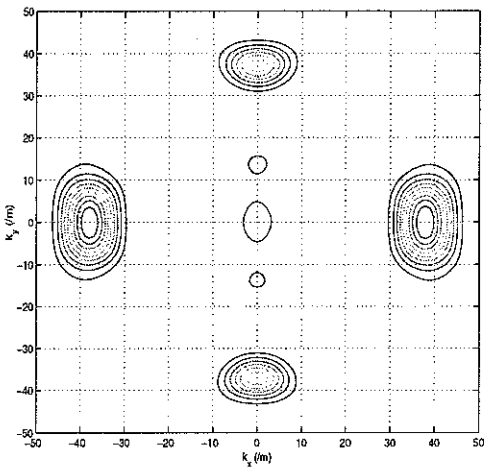

Figure 30. Contribution from all singular values except first two to wavenumber estimation at 500 Hz with centre excitation on simply supported plate with damping loss factor and large area scan.

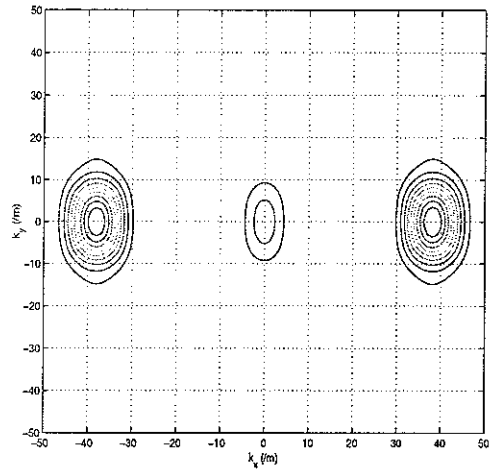

Figure 31. Third singular value contribution to wavenumber estimation at 500 Hz with centre excitation on simply supported plate with damping loss factor and large area scan.

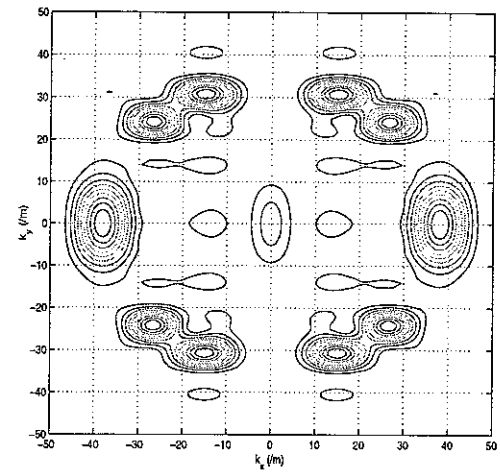

Figure 32. Summation of normalised contribution from first three singular values in estimating wavenumber estimation at 500 Hz with centre excitation on simply supported plate with damping loss factor and large area scan.

4. EXPERIMENTS

4.1. Centre excitation

Experiments were conducted on a curved sandwich panel to validate and compare with some of the findings from previous sections. The panel was hung from a frame using flexible chords. A shaker was attached to the structure through a stinger and was driven by a broadband random signal to excite the structure. To improve the efficiency of measurements and avoid mass loading of the panel, a laser vibrometer has been used to measure the velocities on the surface. Initially shaker attachment location is at the centre of the panel. A PCB 218C force gauge was used measure force input. The scan area used for the first experiment is shown in Figure 33. It is shown projected on to a plane surface. There are 22 points along the X direction, which is the direction of curvature, and 21 along the X direction. The laser beam is expected to hit the panel at an angle larger than that for a plane panel for majority of scan points. Although this will result in measurements that show smaller amplitudes compared to actual velocity, the correction is not applied as the effect is similar to a type of windowing. The correction is, however, made for the distance between scan points accounting for the curvature. Since the

curvature does not allow full area measurement with one set-up, the measurements were made in two stages i.e. left half and right half. Typical measured transfer mobility is shown in Figure 34. The structure shows strong modal behaviour up to around 700 Hz.

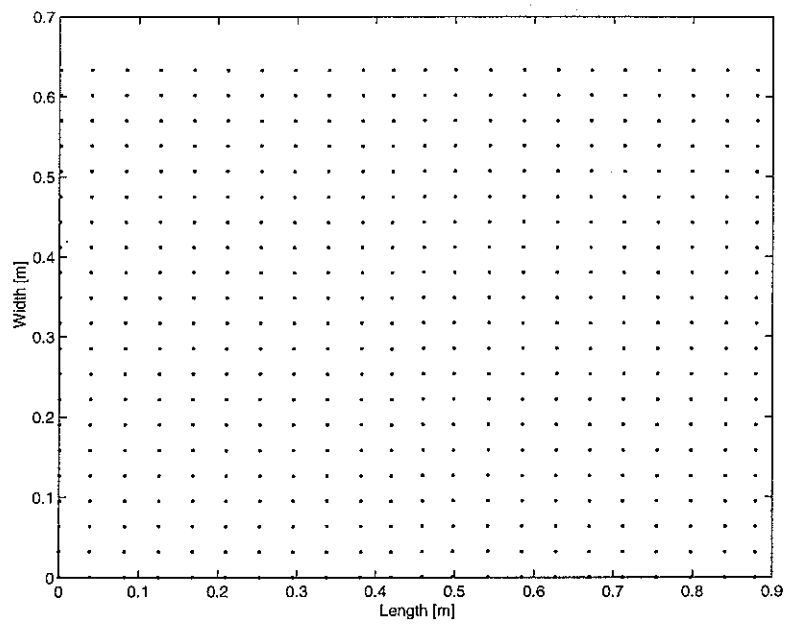

Figure 33. Scan area on curved sandwich panel shown projected on a plane.

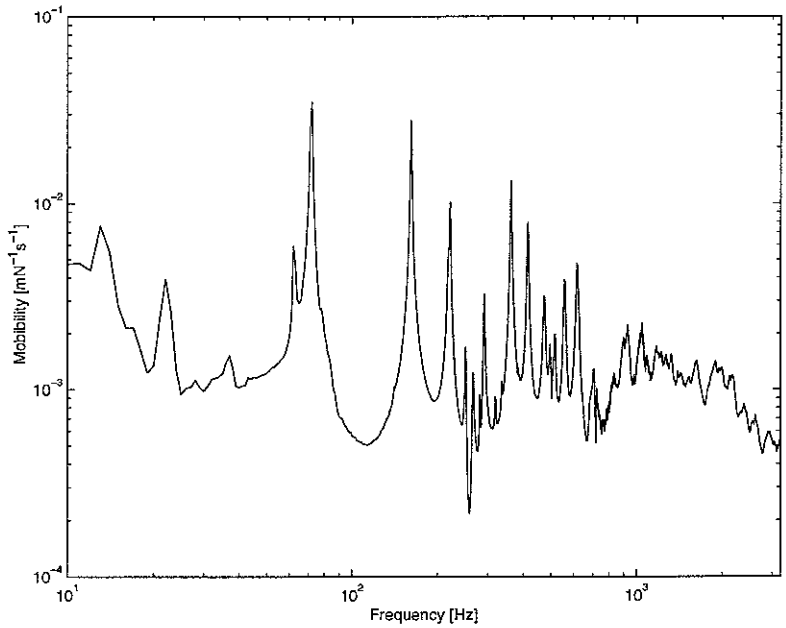

Figure 34. Typical measured transfer mobility on curved sandwich plate.

The singular values of measured FRF matrix are shown in Figure 35. Notice the difference between the variations in Figures in 35 and 21. Since here the matrix is constructed using measured mobilities, singular values tend to a constant value with increasing frequency. The measurement noise level appears to be large at high frequencies. The panel has its first natural frequency at approximately 72 Hz. Below this frequency noise contaminates the measurements.

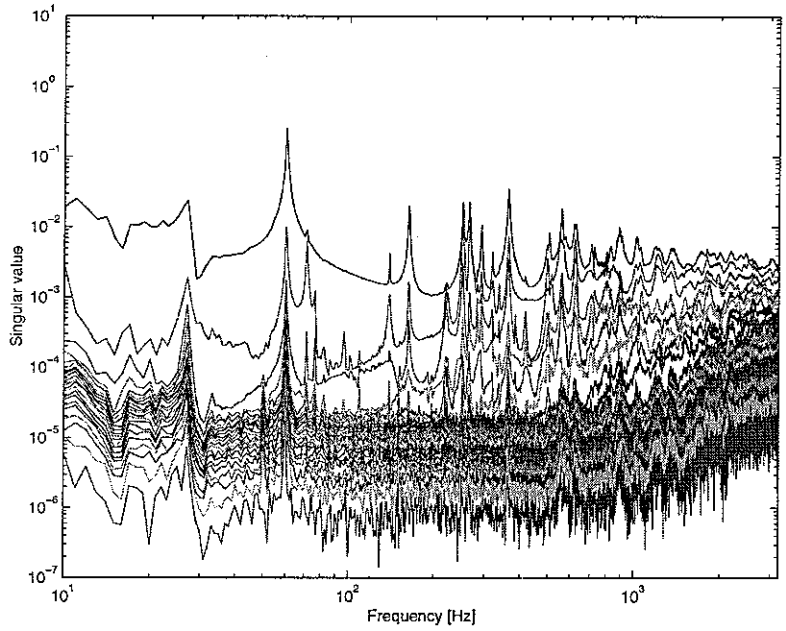

Figure 35. Singular values of mobility matrix of curved sandwich panel excited at the centre.

Using the experimental data, wavenumbers were estimated at 72 Hz, 500 Hz, 1000 Hz, 1200 Hz and 2000 Hz. Figure 36 shows wavenumber estimation at 72 Hz using the full mobility matrix i.e. contributions from all singular values are included. The process identifies definite correlation peaks at two locations only. This is explained by dominance of the first singular value at 72 Hz as seen in Figure 35. This is also confirmed by wavenumber estimation using partial mobility matrix contributed by the first singular value as shown in Figure 37. Two similar locations of contour centres are identified here. The wavenumber information of the second singular value is shown in Figure 38, where four more correlation contours are identified. The third singular value appears to contain wave information, Figure 39, that does not match with the wavenumbers in Figures 37 and 38. This can be attributed to the presence of

side lobes for scan areas covering less than half the wavelength. The effect of limited resolution can also be seen in Figures 37 and 38. In these figures, due to coarser wavenumber resolution, it is difficult to identify directional variation of the wavenumber that is expected due to the curvature effect. Since curvature runs along the X direction, wavenumbers should increase in that direction.

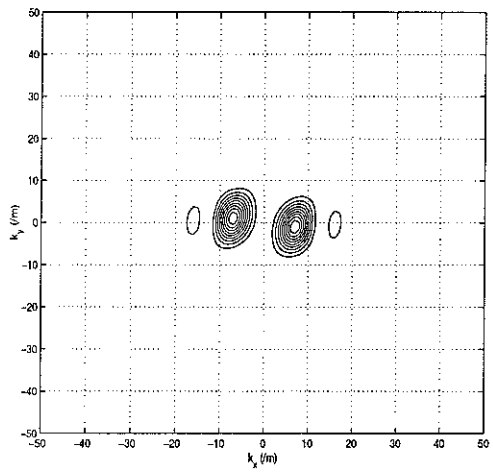

Figure 36. Wavenumber estimation at 72 Hz with centre excitation on curved sandwich panel.

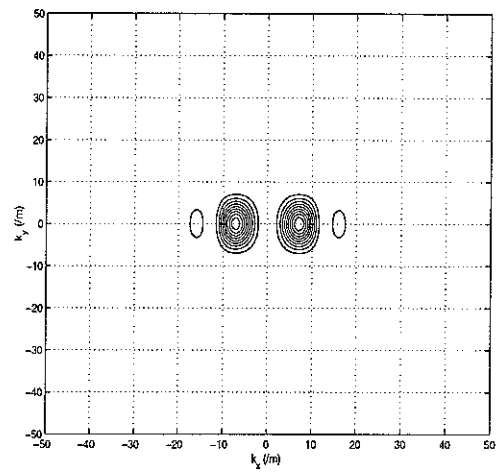

Figure 37. First singular value contribution to wavenumber estimation at 72 Hz with centre excitation on curved sandwich panel.

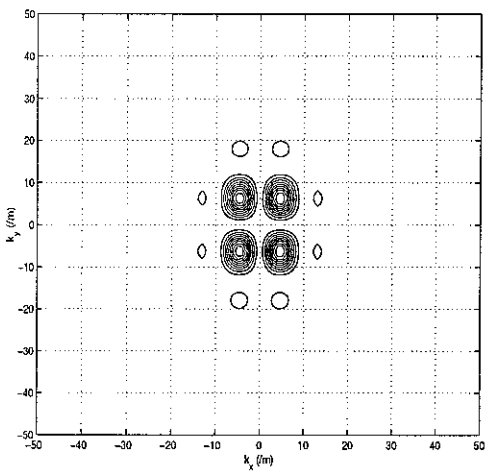

Figure 38. Second singular value contribution to wavenumber estimation at 72 Hz with centre excitation on curved sandwich panel.

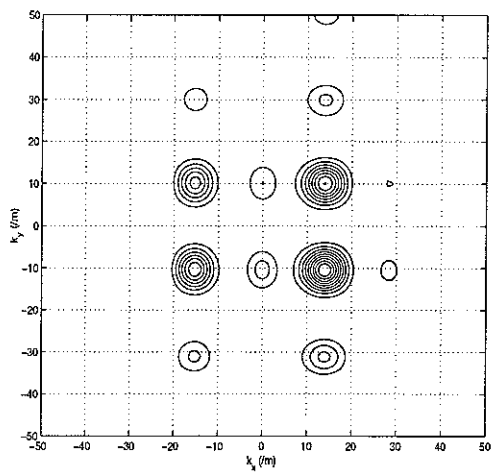

Figure 39. Third singular value contribution to wavenumber estimation at 72 Hz with centre excitation on curved sandwich panel.

Figure 40 shows wavenumber estimation at 500 Hz. More numbers of contours are identified here compared to Figure 36. However, a large number of the wave propagation directions are still missing. Use of singular value decomposition at this frequency might help in identifying a few more wavenumbers. The contribution of the first singular value is shown in Figure 41. Four wavenumbers are identified in this case. The contribution of all singular values except the first is shown in Figure 42. This shows the presence of at least six more wave propagation directions that are identifiable. Wavenumber estimations for contributions from the second and third singular values are shown in Figure 43 and 44. The combined effect of the first three singular values is shown in Figure 45. Comparing Figure 45 with Figure 40, more propagation directions are identified using singular value decomposition. The curvature effect also becomes clearer in Figure 45, where wavenumbers vary from minimum 15 rad/m in the X direction to nearly 10 rad/m in the Y direction.

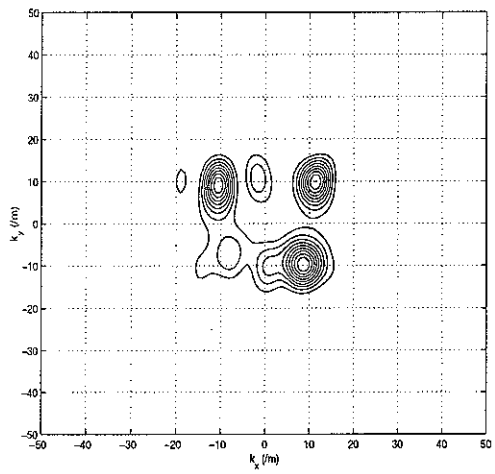

Figure 40. Wavenumber estimation at 500 Hz with centre excitation on curved sandwich panel.

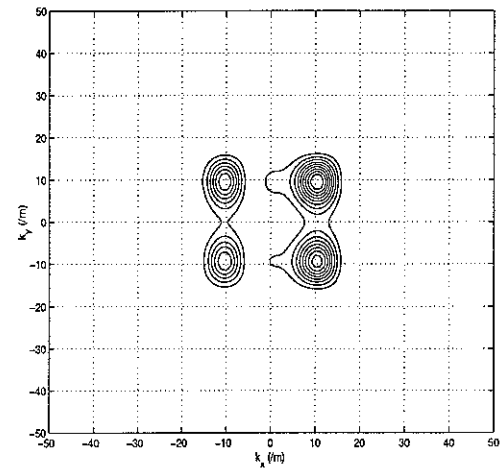

Figure 41. First singular value contribution to wavenumber estimation at 500 Hz with centre excitation on curved sandwich panel.

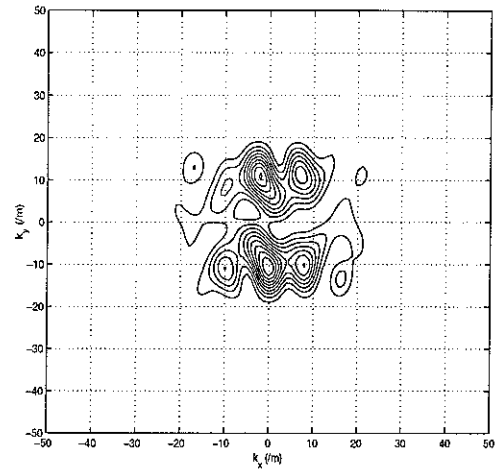

Figure 42. Contribution from all singular values except first one to wavenumber estimation at 500 Hz with centre excitation on curved sandwich panel.

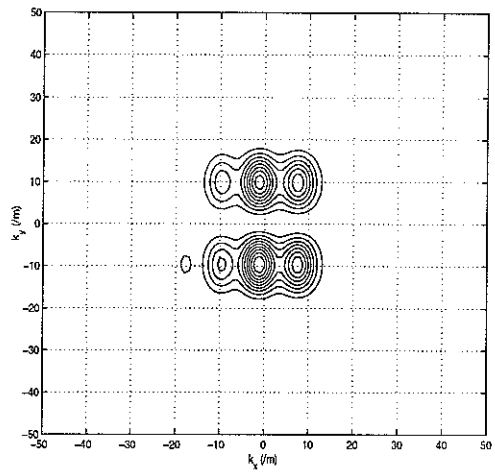

Figure 43. Second singular value contribution to wavenumber estimation at 500 Hz with centre excitation on curved sandwich panel.

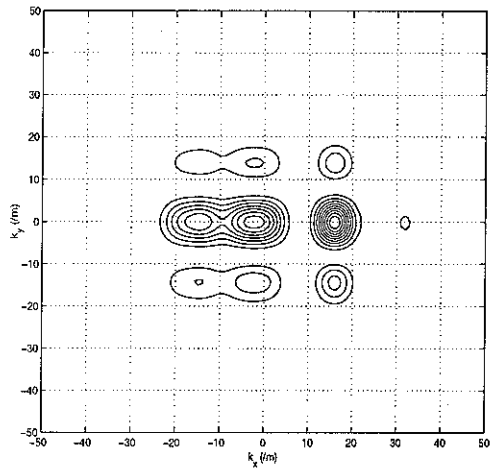

Figure 44. Third singular value contribution to wavenumber estimation at 500 Hz with centre excitation on curved sandwich panel.

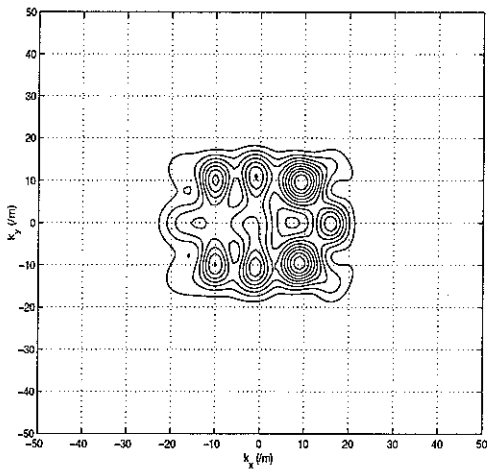

Figure 45. Summation of normalised contribution from first three singular values in estimating wavenumber estimation at 500 Hz with centre excitation on curved sandwich panel.

The wavenumber estimations at some higher frequencies are also shown in Figures 46-51. Above 1000 Hz, SVD may not result in significant additional information for centre excitation for all the cases considered. However, by applying SVD no information is lost. It is also clear from these figures that there is a diminishing effect of curvature on the

directional variation of wavenumbers at higher frequencies. At 2000 Hz wavenumbers estimated are almost equal in amplitude in all of the directions considered.

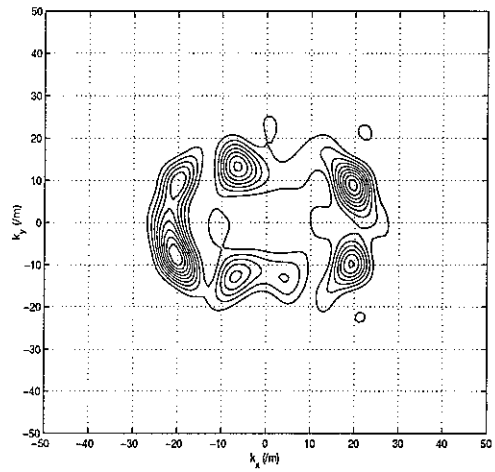

Figure 46. Wavenumber estimation at 1000 Hz with centre excitation on curved sandwich panel.

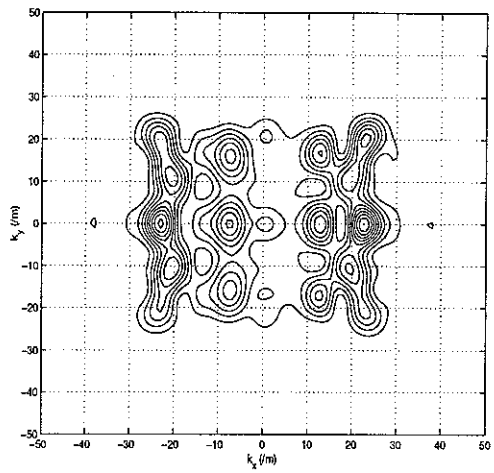

Figure 47. Summation of normalised contribution from first three singular values in estimating wavenumber estimation at 1000 Hz with centre excitation on curved sandwich panel.

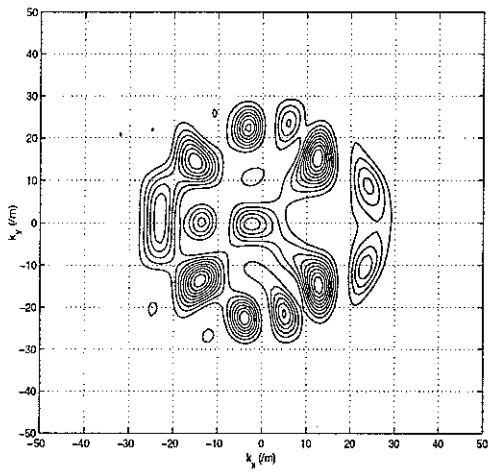

Figure 48. Wavenumber estimation at 1200 Hz with centre excitation on curved sandwich panel.

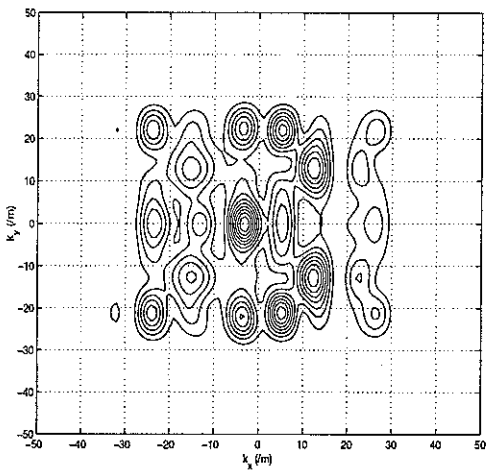

Figure 49. Summation of normalised contribution from first three singular values in estimating wavenumber estimation at 1200 Hz with centre excitation on curved sandwich panel.

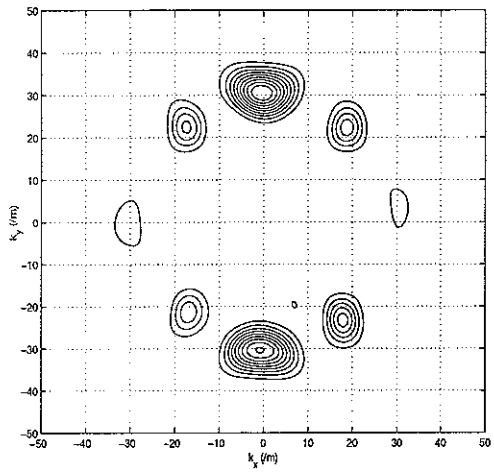

Figure 50. Wavenumber estimation at 2000 Hz with centre excitation on curved sandwich panel.

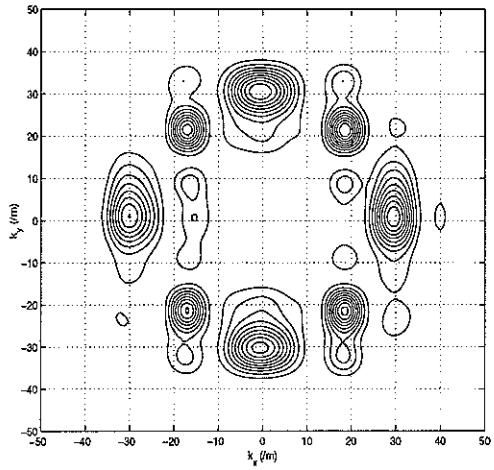

Figure 51. Summation of normalised contribution from first three singular values in estimating wavenumber estimation at 2000 Hz with centre excitation on curved sandwich panel.

4.2. Corner excitation

Experiments were also carried out with corner excitation. The wavenumber estimations at 500 and 1000 Hz are shown in Figures 52-55. Some amount of extra information appears to be extracted due to finer resolution in wavenumbers compared to centre excitation, which is clear from comparison of Figures 52, 54 and 40,46 respectively. This confirms the simulation on a rectangular flat plate. The SVD application appears to improve directional resolution significantly compared to centre excitation (Figure 53).

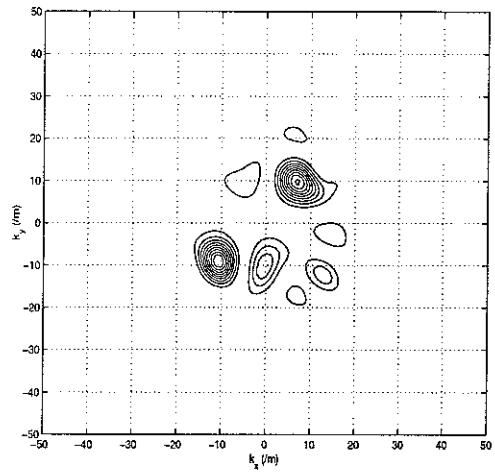

Figure 52. Wavenumber estimation at 500 Hz with corner excitation on curved sandwich panel.

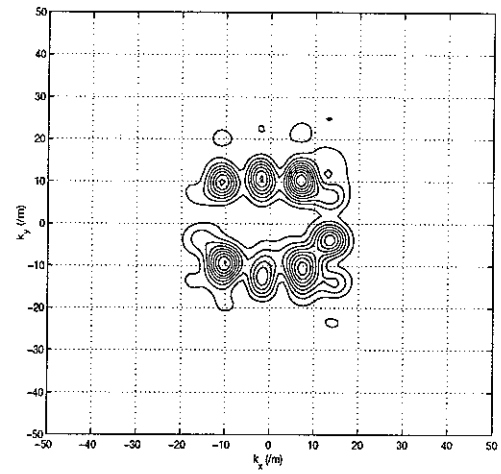

Figure 53. Summation of normalised contribution from first three singular values in estimating wavenumber estimation at 500 Hz with corner excitation on curved sandwich panel.

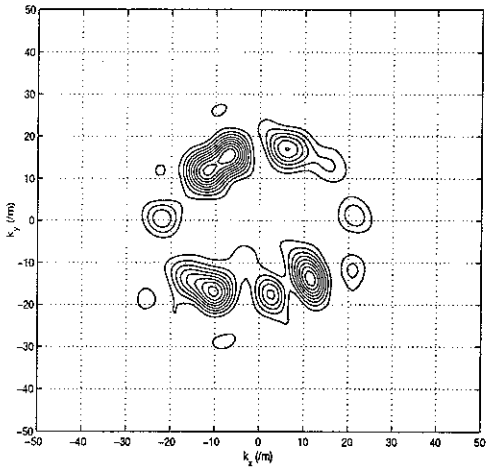

Figure 54. Wavenumber estimation at 1000 Hz with corner excitation on curved sandwich panel.

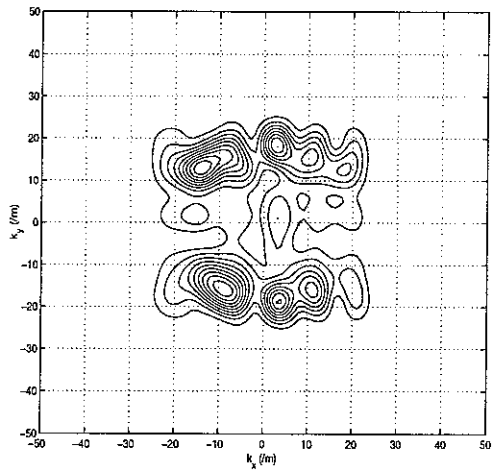

Figure 55. Summation of normalised contribution from first three singular values in estimating wavenumber estimation at 1000 Hz with corner excitation on curved sandwich panel.

5. IMPROVED RESOLUTION OF WAVE PROPGATION DIRECTIONS USING AN ALTERNATIVE APPROACH

As discussed in the previous sections, provided satisfactory wavenumber resolution existed, the predominant wavenumber is estimated accurately by the correlation technique. However, due to varying number of points crossed in different directions of propagations a weighting is applied to the correlation coefficient in the calculations using equation (2). This results in masking of several wavenumbers in different directions. If equation (1) is slightly modified to enable processing in isolated directions of wave propagations, it may be possible to improve directional resolution. The modified correlation coefficient can be written as

$$\hat{W}(k,\theta,\omega)=\int_{-l_x/2}^{l_x/2}\int_{-l_y/2}^{l_y/2} w(x,y,\omega)\,e^{-ik\cos(\theta)x}\,e^{-ik\sin(\theta)y}\,dxdy \tag{7}$$

For sampled data it can be implemented as

$$\hat{W}(k,\theta,\omega)\cong\frac{l_x l_y}{N^2}\sum_{p=1}^{N}\sum_{q=1}^{N} w(x_p,y_q,\omega)e^{-ik\cos(\theta)x_p}\,e^{-ik\sin(\theta)y_q} \tag{8}$$

In the above equation, although every scan point is checked for correlation, only few points contribute significantly to the correlation coefficient. In some directions, the number of scan points significantly contributing is much reduced to that the correlation coefficient might be masked by noise floor and spurious wavenumbers are estimated. Expected smooth variation of wavenumbers with angle θ, provided large number directions are chosen for analysis, can be taken as a guideline in isolating spurious wavenumbers. Effectively the correlation function in equation (1) and (8) is just a function of wavenumber k i.e. estimation of the wavenumber magnitude for specified θ. It may be possible to automate the process by a properly defined algorithm in rejecting spurious wavenumbers. The data generated in section 2, is used here to validate this modification.

The two cases considered here are the large scan area on a flat plate, using either corner excitation with low damping or centre excitation with high damping. Figures 56-59 show wavenumbers estimated at 500 Hz and 800 Hz using above technique. Each dot indicates an identified wavenumber. Comparing Figure 56 with Figure 6 for corner excitation at 500 Hz, a first observation is that more directions of wave propagations are identified. The only limitation being wavenumber resolution that is dependent on scan area. It is more evident in the y

direction as the scan dimension in that direction is very small (less than 0.6 m). For centre excitation, the resolution is much poorer as only half the scan dimension can be used for calculation. This significantly affects wavenumber estimation as shown in Figure 57. At 800 Hz, again a larger number of directions are identified for centre excitation (Figure 59), curiously many missing for corner excitation (Figure 58).

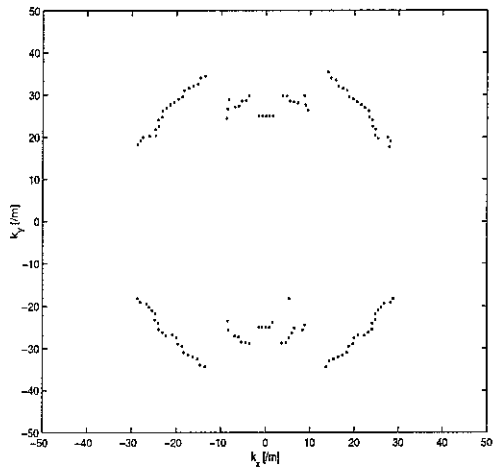

Figure 56. Wavenumber estimation at 500 Hz with corner excitation and large scan area. Damping loss factor is 1%.

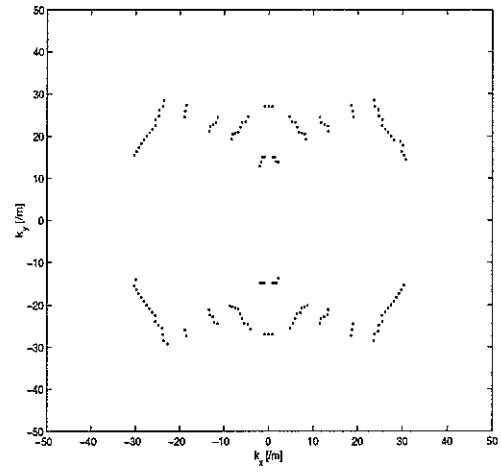

Figure 57. Wavenumber estimation at 500 Hz with centre excitation and large scan area. Damping loss factor is 10%.

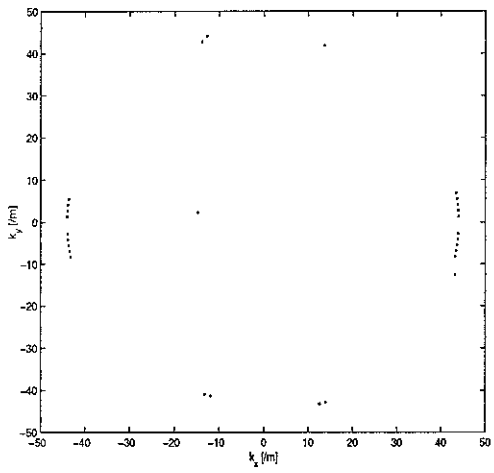

Figure 58. Wavenumber estimation at 800 Hz with corner excitation and large scan area. Damping loss factor is 1%.

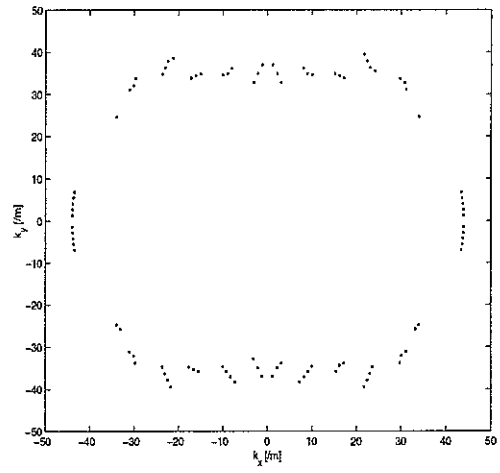

Figure 59. Wavenumber estimation at 800 Hz with centre excitation and large scan area. Damping loss factor is 10%.

This modification to the original formulation appears to have potential in resolving more directions of wave propagation than the original one. But it needs further study and may be combining with SVD for rejecting spurious estimate of wavenumbers.

6. CONCLUSIONS

Numerical experiments were performed on simply supported and free-free supported rectangular flat plates to further study the correlation technique. Different 'measurement' plans were investigated for their performance in improving the identification of wavenumbers in particular directions. Later the singular value decomposition technique was introduced to resolve more directions of wave propagations. Also, the formulation was implemented in polar co-ordinates (section 5). For the validation purpose, some experiments were performed on a curved sandwich panel. The following are some of the conclusions of the study.

a) The measurement procedure using central excitation with large damping provides similar weighting to all directions of wave propagations. Provided the wave number resolution is fine enough, this arrangement should result in a greater number of wavenumbers being identified.
b) Apart from damping and excitation position, the wavenumber resolution is critical in estimating more wavenumbers in the measurements.
c) The application of singular value decomposition technique has been found to improve directional resolution of wavenumbers. It was seen to be effective in both low and high modal overlaps.
d) The polar co-ordinate implementation appears promising provided the wavenumber resolution is fine enough.

It might therefore be possible to combine the effectiveness of SVD and polar co-ordinate implementation, so as to achieve an overall improvement.

7. REFERENCES

1. K. Grosh and E.G. Williams. *Complex wavenumber decomposition of structural vibrations.* Journal of the Acoustical Society of America, Vol. 93, No. 2, (1993), pp. 836-848.
2. J.G. McDaniel and W.S. Shepard Jr. *Estimation of structural wavenumbers from spatially sparse response measurements*. Journal of the Acoustical Society of America, Vol. 108, No. 4, (2000), pp. 1674-1682.
3. J.G. McDaniel, P. Dupont and L. Salvino. *A wave approach to estimating frequency dependent damping and transient loading*. Journal of Sound and Vibration, Vol. 231, No. 2, (2000), pp. 433-449.
4. J.S. Bolton, H.J. Song and Y.K. Kim. *The wavenumber decomposition approach to the analysis of tire vibration. Proc. NoiseCon 98, Ypsilati,* Michagon (1998), pp 97-102.
5. J.S. Bolton and Y-J. Kim. *Wavenumber domain representation of tire vibration. Proc. InterNoise 2000, Nice*, France (2000).
6. N Ferguson, R Halkyard and B Mace, *Estimation of wavenumber in two-dimensional structures, Proc. of ISMA2002*, KUL, Leuven September 2002.
7. K.H. Heron. *Predictive SEA and anisotropic panels, Proc. of ISMA2002*, KUL, Leuven September 2002.